ELSEVIER

Journal of Crystal Growth 240 (2002) 321–329

JOURNAL OF CRYSTAL GROWTH

www.elsevier.com/locate/jcrysgro

The study of light yield increase after low dose rate irradiation in Y^{3+} doping $PbWO_4$ crystals ☆

Xin Zhang*, Jingying Liao, Peijun Li, Hui Yuan, Binfu Sheng, Peifa Shao, Changquan Li, Zhiwen Yin

Shanghai Institute of Ceramics, Chinese Academy of Sciences, Dingxi Road, Shanghai 200050, China

Received 24 July 2001; accepted 22 January 2002
Communicated by R. James

Abstract

Although trivalent ions (such as La^{3+}, Lu^{3+} and Y^{3+}) doping can significantly improve the radiation hardness of lead tungstate crystals, some Y^{3+} doping $PbWO_4$ (PWO) crystals showed exceptional irradiation behavior, namely, light yield increase after low dose rate irradiation. In addition the radiation hardness was sensitive to annealing temperature. In this study, we chose typical Y^{3+} doping crystal samples and investigated the relationship between transmission, light yield and radiation hardness. The experimental results show that high temperature annealing can enhance the absorption band around 430 nm, while annealing at 50°C produces different results and can suppress this exceptional behavior. Light output increase not only exists in the top side of the boule, but also in the seed side, and is accompanied with optical transmission change in the wavelengths from 380 nm to about 500 nm simultaneously. The pre-existing 430 nm color centers in as-grown PWO:Y^{3+} or annealing induced ones are unstable and can be "bleached" by low dose rate irradiation. The results of annealing and irradiation experiments of the samples show that the radiation hardness phenomenon was sensitive to annealing temperature, and thus a proper annealing temperature for PWO crystals was determined.

PACS: 29.40.−n

Keywords: A1. Doping; A2. Bridgman technique; B1. Lead tungstate; B2. Scintillator

1. Introduction

In the past decade, $PbWO_4$ crystals (PWO) have been intensively investigated because they were the scintillator of choice for detectors of the LHC at CERN [1–3]. The scintillation properties and radiation hardness were of particular importance. The photoluminescence spectra of PWO are composed of two components—the blue one peaking at 420 nm and the green one at 480–520 nm.The two PL peaks ascribed to regular WO_4 group and defect associated WO_3 centers, respectively [4,5]. Recent results [6,7] show that the green component originates from the "WO_4+O_i"

☆This work was supported by The National Nature Science Foundation of China (No. 59932002).

*Corresponding author. Tel.: +86-021-6251-2990; fax: +86-021-6251-3903.

E-mail address: xin_zhang30@yahoo.com.cn (X. Zhang).

0022-0248/02/$ - see front matter
PII: S0022-0248(02)00881-3

centers. The radiation hardness of PWO crystals is crucial because of the severe application environment with unprecedented high levels of radiation [8]. Previous studies have shown that high energy radiation does not influence the scintillation mechanisms of PWO, and the light output degradation is caused by the creation of color centers associated with the absorption bands in the UV and the blue spectral regions [3,9]. The most detrimental absorption band in PWO is at 420 nm, and it overlaps with the prime fast luminescence component—blue band.

Besides raw material purifying and the melt stoichiometrical tuning, doping with trivalent and pentavalent ions such as Y^{3+}, La^{3+}, Lu^{3+} and Nb^{5+} could significantly improve the short wavelength transmission and radiation hardness of PWO single crystals by suppressing the 350 nm intrinsic absorption bands. Although the radiation induced color centers have been extensively studied, the color centers in as-grown PWO:Y^{3+} crystals, as well as the transition of these defects during irradiation and annealing procedures, were given little attention. Similar to the absorption bands mentioned above, the 420 nm absorption band, which is introduced by impurities and different growth or annealing conditions, is also harmful to the scintillation properties of PWO. But compared with radiation induced color centers, which can be effectively annihilated by annealing at 200°C, the 420 nm color centers in as-grown crystals are rather stable even at high temperatures.

Compared with undoped and with other ions doped PWO, some Y^{3+} contained crystals grown by modified Bridgeman method have shown different irradiation behaviors, namely, light yield increased when exposed to low dose rate γ-ray or UV irradiation. This phenomenon was accompanied by a transmission change in the wavelengths from 380 nm to about 500 nm.

In the present paper, the results of sequential annealing treatments of Y^{3+} doping PWO crystals from 50°C to 450°C are reported. Experimental results show that high temperature annealing can enhance the absorption band around 430 nm, while annealing at 50°C can partly suppresses this behavior. The interstitial oxygen ion (O''_i) is responsible for the light yield enhancement after low dose rate irradiation, thus giving useful clues regarding steps to suppress this phenomenon.

2. Samples and experimental methods

The PWO crystals were grown from 5N raw material powders by a modified Bridgman method, and the crystallization direction was parallel to the *c*-axis of the crystal. The samples were chosen from full size tapered crystals for Compact Muon Solenoid experiment with the above-mentioned exceptional irradiation behaviors. The details of the samples are listed in Table 1.

The recipe of annealing and irradiation for samples 509 and 595 is as follows: 300°C for 10 h → ^{60}Co irradiation at 35 rad/h for 70 h → ^{60}Co irradiation at 3500 rad/h for 70 h → 50°C for 24 h → ^{60}Co irradiation at 35 rad/h for 70 h → ^{60}Co irradiation at 3500 rad/h for 46 h. Optical transmission and light yield measurements were followed after each annealing and irradiation step.

For samples 448-2 and 448-6, the annealing procedures were carried out sequentially at 50°C, 100°C, 150°C, 200°C, 250°C, 300°C, 350°C and 450°C in air. The soaking time is 24 h for annealing at 50°C and 10 h for other annealing temperatures. It was known that the color centers induced by UV irradiation are similar to those caused by γ-ray for PWO crystal [10]. Therefore, the irradiation was performed by an UV source, 1000 W high-voltage mercury lamp, for 360 s. It

Table 1
Properties of the samples

Crystal ID	Dopant/amount (at ppm)	Dimension (mm^3)	Remarks
448-2	Y^{3+}/150	26.0 × 25.0 × 80.0	Top
448-6		24.0 × 22.0 × 80.0	Bottom
509-1	Y^{3+}/150	21.0 × 21.0 × 115.0	Top
509-2		21.0 × 21.0 × 115.0	Bottom
595-1	Y^{3+}/150	26.0 × 25.0 × 80.0	Top
595-2		24.0 × 22.0 × 80.0	Bottom

was found that prolonging the exposure to irradiation does not influence the absorption spectra, which means that the dynamic equilibrium between the creation and annihilation of color centers has been reached. Optical absorption spectra were recorded after each annealing and UV irradiation step.

The optical absorption spectra were recorded by a SHIMAZU-2501 spectrophotometer with an accuracy of 0.002 abs. The scintillation light yield at room temperature (20°C) was measured by using a Phillips 2262 photomultiplier tube. A collimated γ-ray source ^{137}Cs was used to excite the samples, and the signals were displayed with a QVT multichannel analyzer. X-ray stimulated luminescence spectra were measured before and after UV irradiation with customized equipment using a steady-state X-ray excitation source (tube with Fe anticathode, 80 kV, 4 mA, emission wavelength from 200 to 700 nm). The concentration of the dopant and impurities in the top and middle part of sample 448 were measured by using an inductively coupled plasma-atomic emission spectroscopy (ICP-AES) method.

3. Experimental results

Figs. 1 and 2 and Tables 2 and 3 show the experimental results of samples 509 and 595 after the annealing and ^{60}Co irradiation procedures. After annealing at 300°C for 10 h, all 509 and 595 samples exhibit a 430 nm absorption band, and the absorption intensity in the top part of the crystal is stronger than that in the bottom part. After being exposed to ^{60}Co irradiation at the dose rate of

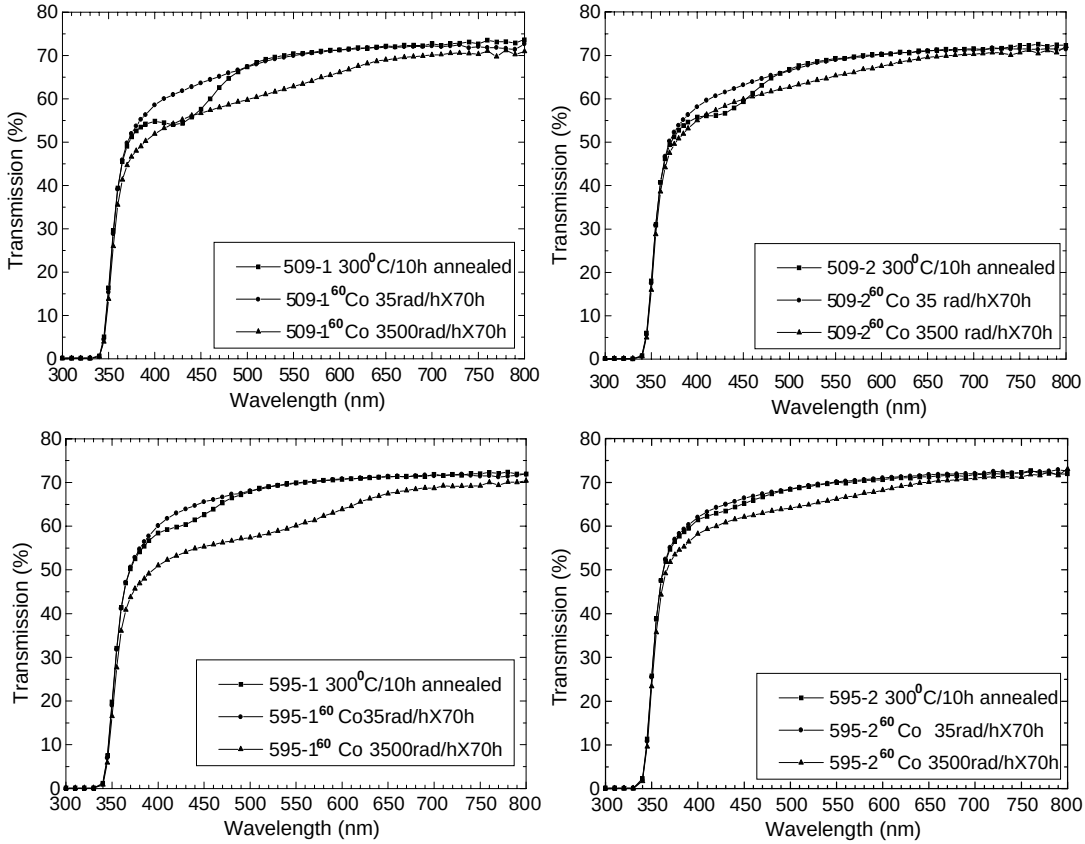

Fig. 1. Transmission spectra of samples 509 and 595 after annealing at 300°C for 10 h and irradiation at different dose rates.

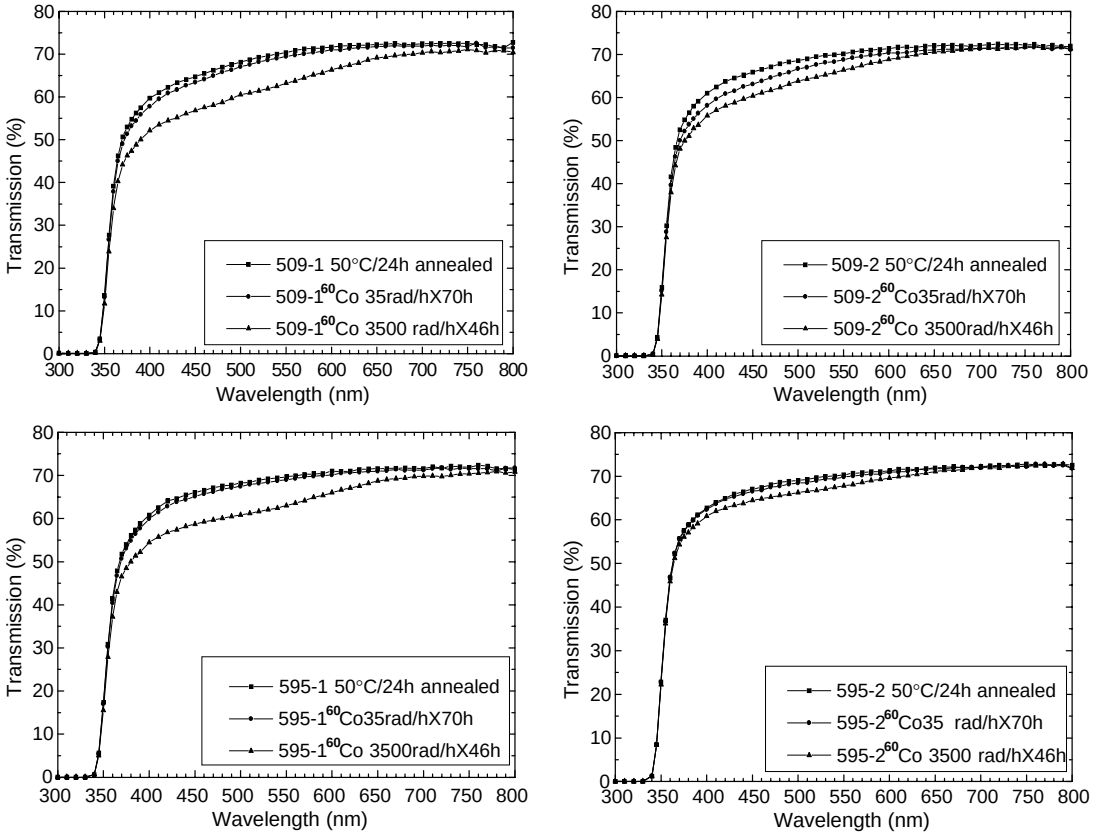

Fig. 2. Transmission spectra of samples 509 and 595 after annealing at 50°C for 24 h and irradiation at different dose rates.

Table 2
The radiation hardness test results of the samples 509 and 595 after being annealed at 300°C for 10 h (Gate: 100 ns, unit: p.e/MeV)

Crystal ID	Light yield after 300°C /10 h annealing	Light yield after ^{60}Co 35 rad/h × 70 h irradiation	Light yield change (%)	Light yield after ^{60}Co 3500 rad/h × 70 h irradiation	Light yield change (%)
509-1	11.5	14.4	+25.4	8.0	−30.3
509-2	13.2	14.9	+13.0	11.4	−13.7
595-1	14.6	16.9	+15.2	7.9	−45.8
595-2	18.6	19.7	+6.3	12.7	−31.6

35 rad/h, this absorption band is "bleached", and it is accompanied by a transmission change around 430 nm and a light yield increase. When exposed to high dose rate irradiation (3500 rad/h), a wide absorption band from 350 nm to about 650 nm was created for all samples, which can also be observed in PWO:Y^{3+} with normal irradiation behaviors. Thus the formation of a wide absorption band which overlaps with the prime fast luminescence component (blue band) results in light yield degradation of Y^{3+}:$PbWO_4$ crystals.

Table 3
The radiation hardness test results of the samples 509 and 595 after being annealed at 50°C for 24 h (Gate: 100 ns, unit: p.e/MeV)

Crystal ID	Light yield after 50°C /24 h annealing	Light yield after ^{60}Co 35 rad/h × 70 h irradiation	Light yield change (%)	Light yield after ^{60}Co 3500 rad/h × 46h irradiation	Light yield change (%)
509-1	12.2	11.9	−2.9	9.6	−21.9
509-2	14.2	13.6	−4.4	11.9	−16.5
595-1	14.5	13.5	−7.4	9.6	−34.3
595-2	18.0	16.7	−7.1	14.1	−21.6

When the samples were annealed at 50°C for 24 h, the absorption band around 430 nm introduced by 300°C annealing attenuates, and the light yield decreases after irradiation for dose rate of 35 and 3500 rad/h.

Fig. 3(a) and (b) exhibit the optical absorption spectra of samples 448-2 and 448-6 after annealing at temperatures from 50°C to 300°C. The change of absorption coefficient around 430 nm can barely be detected when the annealing temperature is higher than 300°C, so the absorption coefficient spectra of 350°C and 450°C annealing are not illustrated in Fig. 3. The absorption coefficient around 430 nm increases as the annealing temperature goes up.

The absorption curves are independent of temperature above about 350°C (illustrated in Fig. 3(a) and (b) as the saturation curve) are the same. The results show that the values of radiation induced absorption coefficient μ are negative around 430 nm. The concentration of color centers created by different procedures can be estimated from optical transmission measurement, since it is proportional to the induced absorption coefficient defined by

$$\mu_{\text{treat}} = 1/d \ln[T_{\text{initial}}/T_{\text{treatment}}],$$

Here, d stands for the thickness of the samples in cm, and T_{initial} and $T_{\text{treatment}}$ are the transmission before and after the treatment procedure, respectively. Fig. 3(c) presents the radiation induced absorption coefficient spectra of 448-6 after the different annealing treatments. The values of the radiation-induced absorption coefficient μ are negative around 430 nm, and positive at 350 and 500 nm. It is an interesting phenomenon that the annealing-induced absorption around 430 nm seems to be effectively "bleached" by UV irradiation. The fact that irradiation attenuates the absorption band around 430 nm while the inverse process can be seen after the annealing procedure, indicating that in this sample the pre-existing or annealing induced 430 nm color centers are unstable.

The ICP-AES analysis results of some impurities (Y^{3+} is the doping ion) in the top and middle part of sample 448 are listed in Table 4. The distribution of Y^{3+} ions is uniform and the high concentration of K^{+} ion is common in PWO crystals, independent of the light yield increases or decreases after low dose rate irradiation. The concentration of Ca^{2+} ions is fairly high at the bottom part, which is consistent with a segregation coefficient of Ca^{2+} ion that is larger than 1.

Fig. 4 presents the X-ray excited emission spectra before and after UV irradiation of sample 448-2 (after annealing at 100°C for 10 h) and 448-6 (after annealing at 300°C for 10 h). The luminescence spectra of the samples show that no new emission peaks appear before and after UV radiation, and the emission intensity increases for wavelengths from 350 to 550 nm. Since the optical transmission deteriorates by high temperature annealing and the saturation absorption curves are almost the same, it is easily deduced that the percentage of light yield change at the bottom part (448-6) is larger than that of the top part (448-2).

In accordance with the results reported in Ref. [11], the emission curves here can be decomposed into four luminescence components (B1, B2, G1 and G2) peaking at 390, 430, 467 and 496 nm, respectively (Fig. 5(a) and (b)). Comparing with

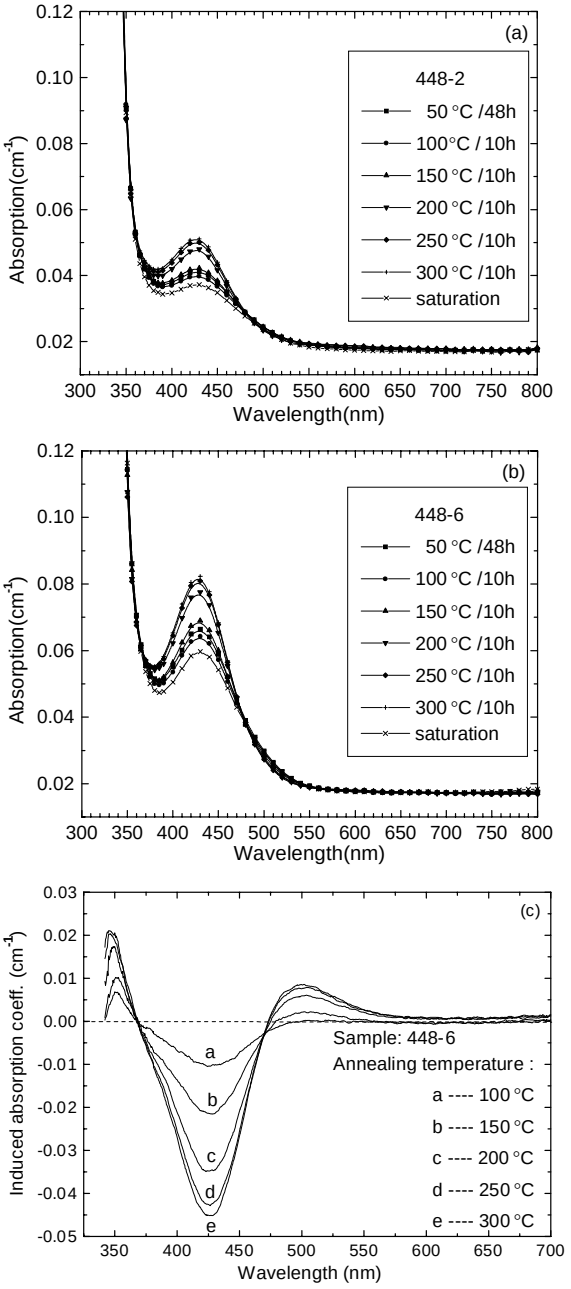

Fig. 3. Absorption and radiation-induced coefficient spectra of 448-2 and 448-6. (a) Absorption spectra of 448-2 after annealing and UV irradiation (b). Absorption spectra of 448-6 after annealing and UV irradiation (c). Radiation-induced absorption coefficient spectra of sample 448-6 at different annealing temperatures.

Table 4
ICP-AES analysis of the concentration of dopant and some impurities in the top and middle part of crystal No.448 (unit: at ppm)

Dopant and impurities	Top part	Middle part
Y^{3+}	93	93
K^{+}	15	7
Ca^{2+}	32	41

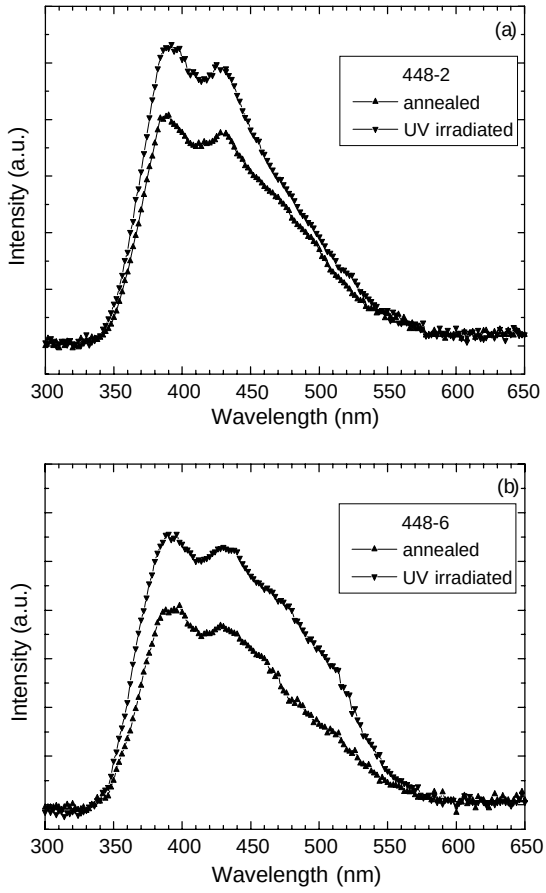

Fig. 4. X-ray excited emission spectra of samples: (a) Emission spectra of sample 448-2 after annealing at 100°C for 10 h and UV irradiation, (b) Emission spectra of sample 448-6 after annealing at 300°C for 10 h and UV irradiation.

Fig. 3(c), the radiation-induced absorption coefficient is positive from 470 nm to about 550 nm, which means the transmission at this band is deteriorated by radiation, but the luminescence

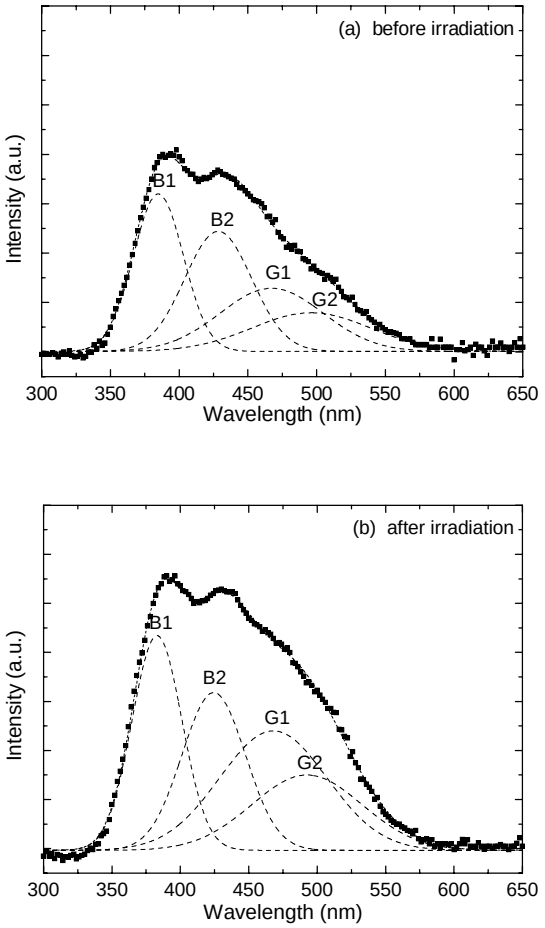

Fig. 5. The Gaussian curve fit results of the X-ray excited emission spectra of samples: (a) Decomposition of 448-6 emission spectrum after annealing at 300°C for 10 h, (b) Decomposition of 448-6 emission spectrum after UV irradiation.

intensity in this band increases. Previous studies have shown that high energy radiation does not influence the scintillation mechanisms of PWO, and the light output degradation is caused by the creation of color centers originating from the absorption bands in the UV and the blue spectral regions [3,9]. In spite of the blue luminescence components, low dose rate irradiation at least enhanced the green scintillation components peaking at 460–500 nm. Therefore, there may be a mechanism that effectively transfers energy of the UV ray to the green luminescence centers. The enhancement of blue scintillation components may relate to the annihilation of 430 nm color centers during irradiation or the same sensitization as the green components, but it is not clear in this study, and further research is needed.

These behaviors of Y^{3+}-doped crystals are different from the experimental results of undoped PWO crystals obtained by Han et al. [12], and they are different from the irradiation results of PWO crystals doped with other ions. According to large-scale experiments that are not discussed in the present paper, this phenomenon only exists in some Y^{3+} or Gd^{3+} [13] doped PWO crystals.

4. Discussion

PWO tends to be "lead deficient" due to the PbO evaporation during the growth procedure [14]. The transition of the 350 nm intrinsic color centers to the 420 nm temporary color centers was observed during the irradiation procedure [12]. In the undoped PWO crystals, besides the V_{Pb}:V_O pairs charge equilibrium mechanism, the "lead deficiency" introduced V_{Pb} (Pb vacancy), which have two effective negative charges relative to the lattice that could be compensated by the defect clusters $[O_2^{3-}–V_{Pb}–V_O–V_{Pb}–O_2^{3-}]$, $[V_F^{-}–V_O–V_F^{-}]$. The defect V_F^{-} in the form of $[V_F^{-}–V_O–V_F^{-}]$ and V_F^0 ($[O_2^{3-}–V_{Pb}–O_2^{3-}]$) causes the 350 and 420 nm absorption bands, respectively [15].

Doping by trivalent ions (such as La^{3+}, Y^{3+}) can markedly enhance the radiation hardness of PWO crystals and suppress the 350 nm intrinsic absorption band. According to computer simulation results of extrinsic defects in PWO [16], the trivalent ions introduce a positive charge defect $(M_{Pb}^{3+})^{\bullet}$, where M^{3+} occupying the Pb sub-lattice was compensated by V_{Pb} in the form of $[2(M_{Pb}^{3+})^{\bullet}–V''_{Pb}]$ (M^{3+} stands for trivalent ions). Integrating the extra V_{Pb} into the defect cluster can avoid the formation of $[V_F^{-}–V_O–V_F^{-}]$ that correlated to the 350 nm absorption band, thus improving the radiation hardness of the crystals. Except for the top part of the crystal, the concentration of Y^{3+} ions is comparatively even because the segregation coefficient of Y^{3+} is close to 1 (0.94 ± 0.04) [17]. The distribution characteristic

of the Y^{3+} ions helps to suppress the defect cluster $[V_F^{\cdot}–V_O–V_F^{\cdot}]$ along the crystal.

PWO crystals grown by modified Bridgman method contain more Y^{3+} ions than those grown by Czochralski methods, even if they were grown from the same raw materials. In addition, the modified Bridgman growth method was carried out in an almost sealed crucible that reduces the PbO evaporation. Reduction of the PbO evaporation has distinct advantages, but leads to V_{Pb} deficiency in Y^{3+} ion doped crystals. Therefore local charge equilibrium modes of Y^{3+} ions may be different along the ingot: in the bottom and the middle part, Y^{3+} ions get V_{Pb} and integrate the defect into the cluster $[2(Y_{Pb}^{3+})^{\bullet}–V''_{Pb}]$. But if the concentration of V_{Pb} was not high enough in the top part, for example, for PWO grown in the almost sealed crucibles, it is possible to form the defect cluster $[2(Y_{Pb}^{3+})^{\bullet}–O''_i]$. The interstitial oxygen ions (O''_i) are considered to be the origin of the light yield increase after low dose rate irradiation [11]. Up-to-date results show that the green component originates from the "WO_4+O_i" centers, and enhancement of the green luminescence component is observed in this study. The analysis mentioned above gives useful clues for eliminating the interstitial oxygen ions (i.e., a proper amount of V_{Pb} is needed for local charge compensation because of the enrichment of Y^{3+} ions at the top part).

In samples 509 and 595, the percentage of light yields increases in the top part is larger than that in the bottom part. It can be explained by the mechanism mentioned above that the defect clusters $[2(Y_{Pb}^{3+})^{\bullet}–O''_i]$ can form near the seed side of the crystals if the concentration of V_{Pb} is too low. It must be mentioned here that the results of samples 509 and 595 agree with the outcomes of the majority of the crystals with increased light yield. On the contrary, in sample 448 the percentage of light yield increases in the bottom part is larger than that in the top part. This newly discovered phenomenon implies that the light yield increase may not relate to impurities in the crystals. In sample 448, it might be correlated with the enrichment of Ca^{2+} ions at the bottom. The radii of Ca^{2+}, Y^{3+} and Pb^{2+} ions are 0.112, 0.102 and 0.129 nm, respectively. From the viewpoint of ion radii, Ca^{2+} ions can occupy the Pb^{2+} sub-lattice easier than Y^{3+}, and moreover, it does not need extra negative charge for equilibrium. The concentrated Ca^{2+} ions at the bottom occupy V_{Pb} site, which are needed for local charge compensation, while the Y^{3+} ions occupy the Pb sub-lattice, thus compelling Y^{3+} to form $[2(Y_{Pb}^{3+})^{\bullet}–O''_i]$.

According to our experiments on V_{Pb} compensator and V_{Pb} creator dopants [18], increasing the amount of V_{Pb} compensator leads to emergence of a prominent 420 nm absorption band, which is unstable under low dose rate irradiation and temperature fluctuations. On the contrary, V_{Pb} creator dopants produce more V_{Pb} needed by the positive charge center-Y_{Pb}^{3+}. Here the Y^{3+} ions occupy the Pb sub-lattice at the top part, thus suppressing the exceptional irradiation behaviors in Y^{3+}-doped PWO crystals. The results of sample 448, together with the evidence of green scintillation increase and experimental results of the V_{Pb} creator dopant, validate the hypothesis that O''_i is responsible for light yield enhancement after low dose rate irradiation, and give useful clues to explain this exceptional behavior in Y^{3+} doped crystals.

5. Conclusion

The pre-existing or annealing induced 430 nm color centers in Y^{3+}:PWO are unstable and can be "bleached" by irradiation. Low dose rate irradiation enhances the green scintillation components peaking at 460–500 nm. The results of annealing and irradiation experiments of the samples reveal that O''_i is responsible for light yield enhancement after low dose rate irradiation, and give useful clues to suppress this phenomenon. Based on this study, experiments on new dopants (which act as a V_{Pb} creator) were carried out to completely eliminate O''_i aiming to produce radiation hard crystals that meet the technical specification established by CMS, CERN.

Acknowledgements

The authors would like to acknowledge helpful assistance on X-ray excited emission spectra

experiments by Prof. Dingzhong Sheng and Master Zekui Li. This work was supported by The National Nature Science Foundation of China (Grant No. 59932002).

References

[1] M. Kobayashi, et al., Nucl. Instrum. Methods 333 (1993) 429.
[2] P. Lecoq, et al., Nucl. Instrum. Methods 365 (1995) 291.
[3] R.Y. Zhu, et al., Nucl. Instrum. Methods 376 (1996) 319.
[4] W. Van Loo, Phys. Status Solidi A 27 (1957) 565.
[5] W. Van Loo, Phys. Status Solidi A 28 (1957) 227.
[6] Shi Caoshu, et al., Chin. Phys. Lett. 328 (2000) 1.
[7] Yonghu Chen, et.al, J. Appl. Phys. 87(3) (2000) 1503.
[8] P.A. Aarnio, et al., Nucl. Instrum. Methods 366 (1993) 98.
[9] E. Auffary et al., Proceedings of the International Conference on Inorganic Scintillators and Their Application, SCINT'95, Delft University Press, Delft, Netherlands, 1995, p. 282.
[10] I. Dafinnei, et al., Proceedings of the International Conference on Inorganic Scintillators and Their Application, SCINT'97 CAS, Shanghai Branch, Shanghai, China, 1997, p. 219.
[11] P. Lecoq, SIC 100 preproduction crystals, Crystal Evaluation group, 26 March 2001.
[12] Baoguo Han, et al., J. Appl. Phys. 86 (7) (1999) 3571.
[13] S. Baccaro, et al., Phys. Status Solidi A 164 (1997) R9.
[14] A. N. Annekov, et al., Phys. Status Solidi A 170 (1998) 47.
[15] Qisheng Ling, et al, Phys. Status Solidi A 181 (2000) R1.
[16] Qisheng Ling, et al, Phys. Status Solidi A, in press.
[17] Qu Xiangdong, Thesis for the degree of doctor of philosophy, Shanghai Institute of Ceramics, Chinese Academy of Sciences, 2001.
[18] Xin Zhang, et al., unpublished results.